

DEVELOPMENT OF A HUMANOID BIPED WALKING ROBOT HUBOT-1 INITIAL DESIGN AND RESULTS ACHIEVED

Nguyen Thanh Nhut, Phan Huynh Lam, Chung Tan Lam

DCSELAB, University of Technology, VNU-HCM

(Manuscript Received on October 21th, 2010, Manuscript Revised January 21st, 2011)

ABSTRACT: *This paper presents an overview of the design process of humanoid robot HUBOT-1: mechanical design, gait planning, control architecture and sensors implementation. The robot is designed with full body in style of Vietnamese body proportion. At the present state the lower limbs with 12 DOF are considered for natural walking pattern from hip and ankle trajectories. Walking pattern based on ZMP criterion. Also, the dead-beat controller of servo motor is implemented for joint control. In addition, the robot used IMU and FSR sensors which are designed and implemented for verifying the ZMP trajectory in stability area.*

Keywords: *biped robot, walking pattern generation, ZMP*

1. INTRODUCTION

Humanoid is one of the most exciting topics in the field of robotics. Humanoid robots are being developed to perform human tasks like personal assistance. They can use tools and operate equipment and vehicles designed for the human form. The motivation of the research is the suitability of the biped structure for tasks in the human environment. The goal of the studies in this area is to reach the human walking dexterity, efficiency, stability, effectiveness, and flexibility. Several different types of humanoid robots have been developed for the last decade: child size robots whose heights are about 120cm have also been developed by Honda (Asimo) and Tokyo University (H6 and H7) [1]. Sony has developed a small toy size robot whose height is only 50cm (SDR-3X) [2]. Heavy adult size robots which are over 180cm in height and

weight over 100kg have been developed by Honda and Waseda University [3]. Also the control of a biped humanoid is a challenging task due to the many degrees of freedom involved and the nonlinear and hard-to-stabilize dynamics [4].

The ZMP criterion is the most widely accepted and used stability measure for the biped robot locomotion. The natural ZMP trajectories for biped robot are presented in [4] which is not discussed in this paper. After having found the required reference trajectories, a position deadbeat control scheme for the robot joints with references joint angles obtained by inverse kinematics of the model.

In this paper, a biped walking robot platform composed of 23 DOF HUBOT-1 is developed, and an off-line motion control of the biped walking robot is implemented taking into account body stability. Also sensors

development is presented for realtime control during walking in the future work. Simulations using Matlab - Simulink are performed of each topic to show the possibility from theory to practical fields.

2.MECHANICAL DESIGN

HUBOT-1 is the first prototype model of DCSELAB. The mechanism is designed to achieve low speed walking at 0.3m/s on the flat floor without obstacles. The power is supplied from outside. Total weight of the humanoid including exterior appearance parts is about 30 kg.

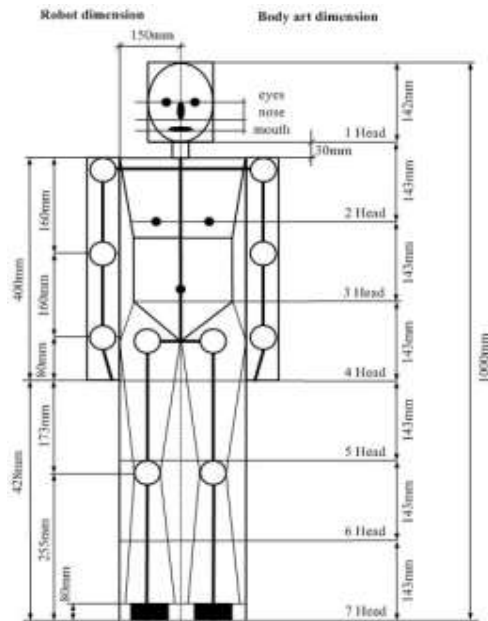


Fig. 1. Vietnamese body proportion

The target motion of HUBOT-1 is that it can imitate several simple forms of human walking motion and stand with hand shaking. We refer to the guideline of Vietnamese body proportion, the 7-head principle is applied, and the overall dimensions of the humanoid robot of 1000mm tall are shown in Fig. 1.

The proposed human proportion is used to design the mechanical parts of HUBOT-1. It is designed with 23 DOF: 12 DOF in legs, 1 DOF in head, and 10 DOF in arms (Table 1). The allocation of joints are shown in Fig. 2. The joint axis of the shoulder, hip, elbow, knee and ankle cross each other for kinematic simplicity and for the dynamic equation of motion [5].

Table 1. The joint allocation

	Joint		No. of Joint	
Head	Yaw		J21	
Arm	Wrist	Yaw	J17,J23	
		Pitch	J18, J24	
	Elbow	Pitch	J16,J22	
		Shoulder	Yaw	J15,J21
			Roll	J14,J20
Leg	Hip	Pitch	J13,J19	
		Roll	J4,J9	
		Yaw	J17,J23	
	Knee	Pitch	J5,J8	
		Ankle	Roll	J2,J11
			Pitch	J1,J12

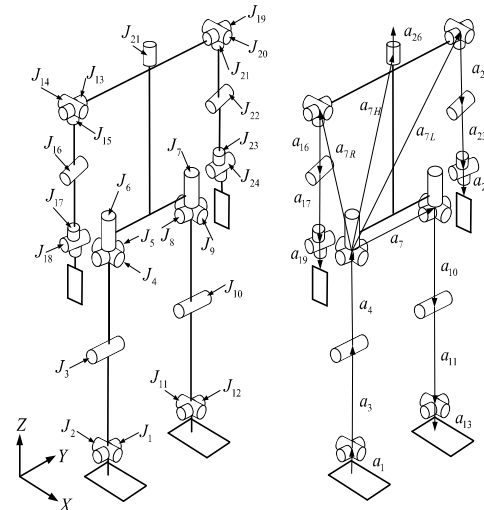


Fig 2. Joint position vectors

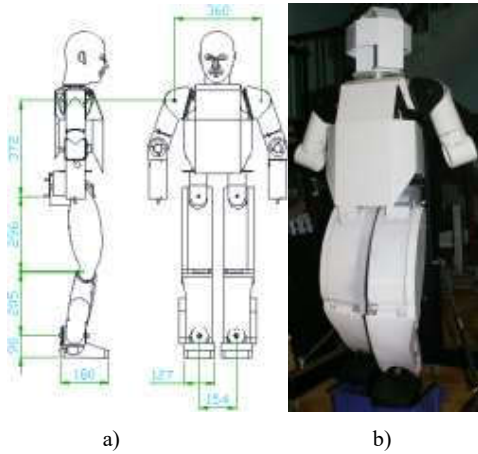


Fig. 3. (a) CAD design of HUBOT-1, (b) Body of HUBOT-1

In the Fig. 3, the body art dimensions is shown on the right, and the length of the limbs of our robot are shown on the left, respectively.

After determining the basic mechanical structure, it is required to design the metallic frames which act as the supporting skeleton of the whole body. The robot is designed by CAE for the trade-off between the stiffness of material and the lightweight of the body. Shape of the frames should be determined to obtain high stiffness under the constraint of minimizing the total weight. We employed FEM-based technique to develop stiff and light frames of the lower body for stable walking. The FEM analysis is an effective method to design the layout of a body in its initial design step to achieve the above objectives.

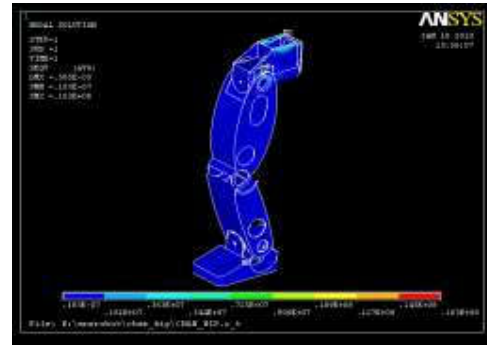


Fig. 4. Results of the FEM analysis for leg

3.GAIT PLANNING

* Humanoid walking analysis

Each foot trajectory can be denoted by a ankle position vector $X_a = [x_a(t), z_a(t), \theta_a(t)]^T$ and hip position vector $X_h = [x_h(t), y_h(t), z_h(t), \theta_h(t)]^T$. When both foot trajectories and the hip trajectory are known, all joint trajectories of the biped robot will be determined by kinematic constraints.

* Ankle motion

The trajectories for the ankles and the orientation of the feet, the trajectories of the feet can be found from kinematic constraints. From [6], we get the following constraints:

$$x_a(t) = \begin{cases} kD_s, & t = kT_c \\ kD_s + l_{an} \sin q_b + l_{af}(1 - \cos q_b), & t = kT_c + T_d \\ kD_s + L_{ao}, & t = kT_c + T_m \\ (k+2)D_s - l_{an} \sin q_f - l_{ab}(1 - \cos q_f), & t = (k+1)T_c \\ (k+2)D_s, & t = (k+1)T_c + T_d \end{cases} \quad (1)$$

$$z_a(t) = \begin{cases} h_{gs}(k) + l_{an}, & t = kT_c \\ h_{gs}(k) + l_{af} \sin q_b + l_{an} \cos q_b, & t = kT_c + T_d \\ H_{ao}, & t = kT_c + T_m \\ h_{gs}(k) + l_{ab} \sin q_f + l_{an} \cos q_f, & t = (k+1)T_c \\ h_{gs}(k) + l_{an}, & t = (k+1)T_c + T_d \end{cases} \quad (2)$$

$$\theta_a(t) = \begin{cases} q_{gs}(k), & t = kT_c \\ q_b, & t = kT_c + T_d \\ -q_f, & t = (k+1)T_c \\ -q_{ge}(k), & t = (k+1)T_c + T_d \end{cases} \quad (3)$$

where

k : number of step

T_c : step period

T_d : the interval of the double-support phase

$kT_c + T_m$: the time of right foot at its highest point

l_{an} : the height of the foot

l_{af} : the length from the ankle joint to the toe

l_{ab} : the length from the ankle joint to the heel

(L_{ao}, H_{ao}) : the highest position of the swing foot.

D_s : the length of one step

$q_{gs}(k), q_{ge}(k)$: the angles of the ground surface under the support foot.

q_b : the angle of foot as it leaves the ground

q_f : the angle of foot as it lands on the ground

*** Hip motion**

The hip motion of the steady phase is determined. The hip motion of the starting phase and the ending phase can be obtained similarly.

Hip motion of $z_h(t)$ hardly affects the position of the ZMP. We can specify $z_h(t)$ to be constant, or to vary within a fixed range.

$$z_h(t) = \begin{cases} H_{h \min} & t = kT_c + 0.5T_d \\ H_{h \max} & t = kT_c + 0.5(T_c - T_d) \\ H_{h \min} & t = (k+1)T_c + 0.5T_d \end{cases} \quad (4)$$

where $H_{h \max}$: highest position of the hip at middle of the single-support phase, $H_{h \min}$: lowest position of the hip at middle of the double-support phase during one walking step.

The change of $x_h(t)$ and $y_h(t)$ is the main factor that affects the stability of a biped robot walking.

$$x_h(t) = \begin{cases} kD_s + x_{ed} & t = kT_c \\ (k+1)D_s - x_{sd} & t = kT_c + T_d \\ (k+1)D_s + x_{ed} & t = (k+1)T_c \end{cases} \quad (5)$$

where x_{sd}, x_{ed} : distances along the x-axis from the hip to the ankle of the support foot at the start and end of the single-support phase, respectively.

It is desirable that hip motion of $\theta_h(t)$ is constant:

$$\theta_h(t) = 0.5\pi \text{ rad} \quad (6)$$

The trajectory of hip and ankle in sagittal plane obtained by third spline interpolation from the second derivative continuity condition and equation (1),(2),(3),(4),(5)&(6), respectively.

In this paper, $y_h(t)$ obtained from natural CoM references presented in [4]

$$y_h(t) = \frac{a_0}{2} + \sum_{k=1}^{\infty} \left[a_k \cos\left(\frac{2\pi kt}{2T_c}\right) + b_k \sin\left(\frac{2\pi kt}{2T_c}\right) \right] \quad (7)$$

the Fourier coefficients of $y_h(t)$ can be obtained as

$$\begin{aligned}
 a_0 &= 0 \\
 a_k &= 0 \\
 b_k &= \frac{2AT_c^2\omega_n^2(1-\cos k\pi)}{k\pi(T_c^2\omega_n^2+k^2\pi^2)}, k=1,2,3,\dots \quad (8) \\
 \omega_n &= \sqrt{g/z_c}
 \end{aligned}$$

In this equation, A is the distance between the foot centers in the y -direction, g is the gravity constant (9.8 m/s^2) and z_c is the height of the plane on which the motion of the point mass is constrained in LIMP model, with this robot model z_c is chosen equal z_h .

Vukobratovic's ZMP criterion [7] is used for balance control. The ZMP can be calculated by using Newton's law from Robot Motion [6] as:

$$\begin{aligned}
 x_{ZMP} &= \frac{\sum_{i=1}^n m_i(\ddot{z}_i + g_z)x_i - \sum_{i=1}^n m_i\ddot{x}_iz_i - \sum_{i=1}^n J_{i,y}\dot{\omega}_{i,y}}{\sum_{i=1}^n m_i(\ddot{z}_i + g_z)} \\
 y_{ZMP} &= \frac{\sum_{i=1}^n m_i(\ddot{z}_i + g_z)y_i - \sum_{i=1}^n m_i\ddot{y}_iz_i + \sum_{i=1}^n J_{i,x}\dot{\omega}_{i,x}}{\sum_{i=1}^n m_i(\ddot{z}_i + g_z)} \quad (9)
 \end{aligned}$$

where n is the number of links, m_i is mass of link i , I_{ix}, I_{iy} is the inertia components of link i , ω_{ix}, ω_{iy} is the absolute angular velocity components around x -axis and y -axis at center of gravity of link i , g_z is the gravitational acceleration, (x_i, y_i, z_i) is the coordinate of the mass center of link i on origin coordinate system. If the ZMP is within the convex hull of all contact points (the stable region), the biped robot is able to walk.

By chance x_{sd}, x_{ed} we obtain desired trajectories with a large stability margin.

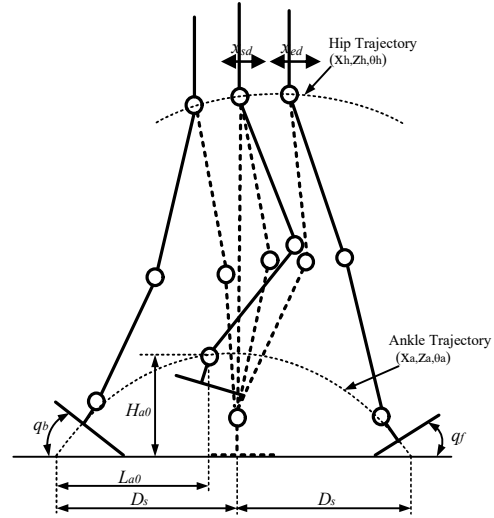


Fig. 5. Gait planning [6]

*Control strategy

Fig. 6 schematically presents the developed control strategy. The control strategy is composed of two parts: offline motion planning and static dynamics control to legs. The motion planning is based on a ZMP criterion to determine the body trajectory as described. Lastly, inverse kinematics is applied for the transformation of the ankle and body trajectories into joint angular trajectories.

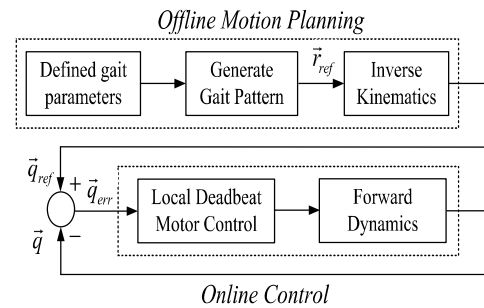


Fig. 6. Control strategy of offline motion planning and static dynamic control.

The gait trajectory planning and simulation using Matlab is shown in Fig. 7, and

the number of parameters that completely describes the desired gait parameters for the simulation, in Table 2, respectively.

The dynamic simulation using Matlab - Simmechanics connect to Solidworks for full-dynamics 3-D simulation. This simulation permits easy calculation of the required actuators' torques.

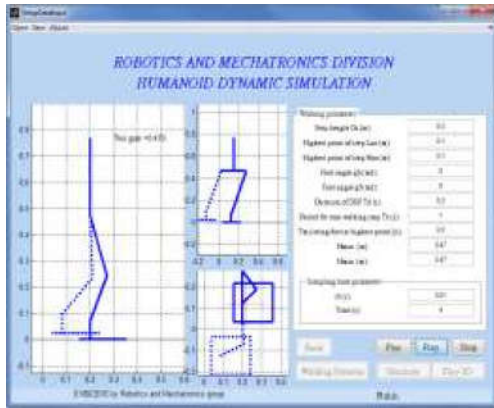
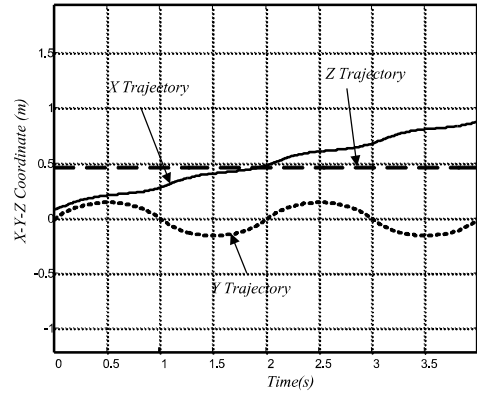


Fig. 7. Simulation interface

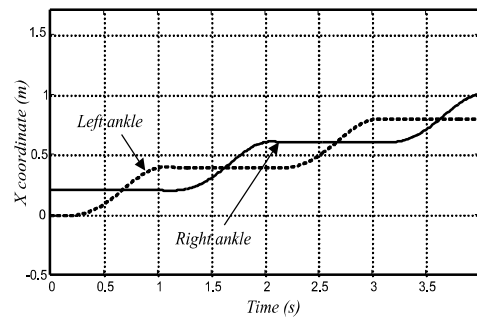
Table 2. The parameters for the foot simulation

Motion Parameters	Value
Number of step, k	4
Step period, T_c	1s
SSP/DSP ratio, r	4
Duration of SSP, T_s	0.8s
Step length, D_s	0.2m
Highest point of step (L_{ao}, H_{ao})	(0.1,0.1)m
Foot angle, q_b and q_f	0, 0
Ground angle, q_{gs} and q_{ge}	0 (level ground)
Dimension parameters	
Ankle height, l_{an}	0.074m

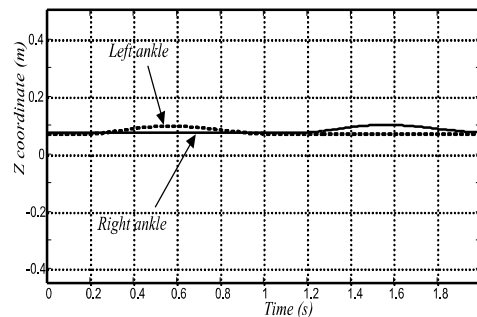
Rear foot length, l_{af}	0.158m
Front foot length, l_{ab}	0.044m
Distance between the foot centers in the y-direction A	0.25m



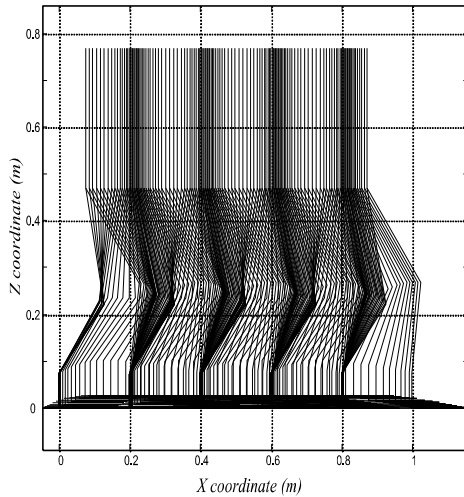
(a) Hip trajectory



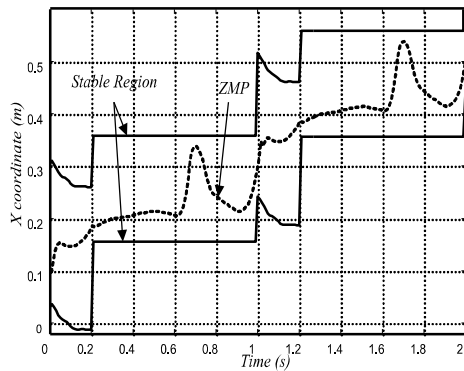
(b) Foot motion in x-axis



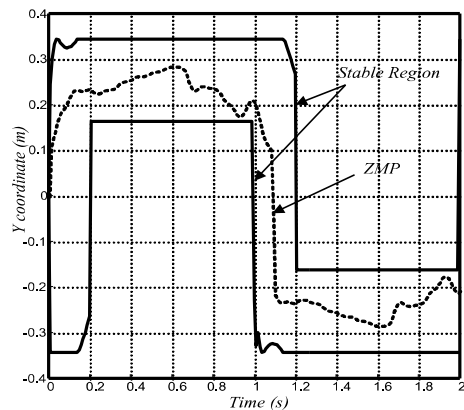
(c) Foot motion in z-axis



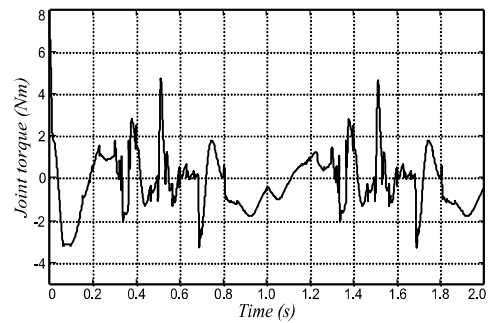
(d) Full body trajectory



(e) ZMP trajectory in x-axis



(f) ZMP trajectory in y-axis



(g) Pitch joint torque of right hip

Fig. 8. Simulation result

Fig. 8 show some results of the simulation. Fig.8.d show the stick picture with $q_b = q_f = 0$. The hip trajectories (Fig. 8.a) and the both foot trajectories (Fig. 8.b,c) are smooth. The ZMP trajectories that satisfy the largest margin is shown in Fig.8.e,f. Fig.8.g show results of the pitch joint torque of right hip as an example. Through the simulations (all of the results are not shown in this paper), it is known that a high foot requires large peak torque and velocity of almost all the joints. Different foot motion can be produced by adjusting the values of the foot constraint parameters. Based on the chosen walking gait, it is also possible to select a walking pattern requiring small specifications of the joint actuators.

4. MOTOR CONTROL

The actuators have been chosen to use two different servo motors for two parts: (1) the legs with servo motors are exposed to high torques since they will be carrying the body during walk and will be exposed to a load during stance; (2) the arms with RC servo motors only have to move their own weight. This research focuses on the walk of the biped and ignoring the effects of the arms. Each arms

weight 1,2kg. It is much less than the 25-kg robot weight.

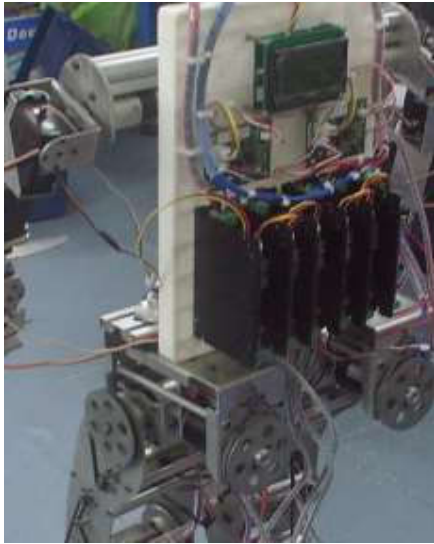


Fig. 9. Motor drivers on testing

The problem of identification consists of estimation of system's model basing on observations of input-output data. It allows to obtain a mathematical model describing dynamical behaviour of the system. The motor system is described as

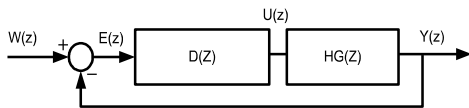


Fig. 1. The system of motor

in which $HG_p(z)$ is the transfer function of the system. With OE model structure, the transfer function is in the form of as

$$HG_p(z) = \frac{Y(z)}{U(z)} = \frac{a_1 z + a_2}{z^2 + b_1 z + b_2} \quad (10)$$

Then the estimation is processed to give a_1, a_2, b_1, b_2 which are the input and output of the system respectively.

As for the experiment of the system on Fig. 9, the model fitting is 69.73% at sampling time of 0.0015s.

The estimated result gives $a_1 = 0.000435$, $a_2 = 0.0004364$, $b_1 = 0.8433$, $b_2 = 0.009029$. The Eq. (11) shows mathematical representation of estimated system for joint motor Harmonic servo motor RH-8-3006-E020A0-SP with 200ppr encoder as follows:

$$HG_p(z) = \frac{0.000435z - 0.0004364}{z^2 - 0.8433z + 0.009029} \quad (11)$$

The dead-beat controller is given by followings:

$$D(z) = \left(\frac{1}{HG_p(z)} \right) \left(\frac{z^{-k}}{1 - z^{-k}} \right) \quad (12)$$

with dead-beat law: $G_m(z) = z^{-k}, k \geq 1$.

The controller give the output as input in some delay. We choose $G_m = z^{-1}$,

$$D(z) = \left(\frac{z^2 + b_1 z + b_2}{a_1 z + a_2} \right) \left(\frac{z^{-1}}{1 - z^{-1}} \right)$$

$$\Rightarrow D(z) = \left(\frac{z + b_1 + b_2 z^{-1}}{a_1 z + (a_2 - a_1) - a_2 z^{-1}} \right)$$

we have:

$$D(z) = \left(\frac{\frac{1}{a_1} + \frac{b_1}{a_1} z^{-1} + \frac{b_2}{a_1} z^{-2}}{1 + \frac{a_2 - a_1}{a_1} z^{-1} - \frac{a_2}{a_1} z^{-2}} \right) \quad (13)$$

$$\Rightarrow D(z) = \left(\frac{\alpha_1 + \alpha_2 z^{-1} + \alpha_3 z^{-2}}{1 + \beta_1 z^{-1} - \beta_2 z^{-2}} \right) \quad (14)$$

$$\alpha_1 = \frac{1}{a_1}; \alpha_2 = \frac{b_1}{a_1}; \alpha_3 = \frac{b_2}{a_1}; \beta_1 = \frac{a_2 - a_1}{a_1}; \beta_2 = \frac{a_2}{a_1}$$

$$D(z) = \frac{U(z)}{E(z)} = \frac{\alpha_1 + \alpha_2 z^{-1} + \alpha_3 z^{-2}}{1 + \beta_1 z^{-1} - \beta_2 z^{-2}}$$

$$\Rightarrow U(z) + \beta_1 U(z)z^{-1} - \beta_2 U(z)z^{-2} = \alpha_1 E(z) + \alpha_2 E(z)z^{-1} + \alpha_3 E(z)z^{-2}$$

$$\Rightarrow U(z) = \alpha_1 E(z) + \alpha_2 E(z)z^{-1} + \alpha_3 E(z)z^{-2} - \beta_1 U(z)z^{-1} + \beta_2 U(z)z^{-2}$$

Applying differential operation on Eq. (8), we have the controller is the following:

$$u_k = \alpha_1 e_k + \alpha_2 e_{k-1} + \alpha_3 e_{k-2} - \beta_1 u_{k-1} + \beta_2 u_{k-2} \quad (15)$$

As for the implementation on motor RH-8-3006-E020A0-SP; the system identification process give the following results:

The motor transfer function is

$$HG_p(z) = \frac{0.000435z - 0.0004364}{z^2 - 0.8433z + 0.009029} \quad (16)$$

and the coefficients of (13) is as follows:

$$\begin{aligned} \alpha_1 &= 2298.850574712644 \\ \alpha_2 &= -1938.620689655173 \\ \alpha_3 &= 20.756321839080460 \\ \beta_1 &= -2.003218390804598 \\ \beta_2 &= -1.003218390804598 \end{aligned} \quad (17)$$

5. SENSORS IMPLEMENTATION

To provide feedback for the controller a number of sensors are available on HUBOT-1: Force Sensing Registers (FSR) and Inertial Measurement Unit sensor (IMU sensor). The FSR provide measurements of forces from each foot which can be used for CoP (center of pressure) position sensing. In a balanced gait, the ZMP coincides with CoP [7]. The ZMP in SSP is calculated as follows:

$$P_{ZMP} = P_{CoP} = \frac{\sum_{j=1}^N p_j f_{jz}}{\sum_{j=1}^N f_{jz}} \quad (18)$$

where N is the number of FSR sensors on the foot, f_{jz} is the force applied on sensor j in z -direction, and p_j is the position of sensor j .

If the biped robot is in DSP, the ZMP can be found by interpolation the ZMP calculated for each foot, and weighing by the total force applied to all the sensors:

$$P_{ZMP} = \frac{\sum_{j=1}^{N_r} p_{jr} f_{jzr} + \sum_{j=1}^{N_l} p_{jl} f_{jzl}}{\sum_{j=1}^{N_r} f_{jzr} + \sum_{j=1}^{N_l} f_{jzl}} \quad (19)$$

where N_r and N_l are the total number of sensor on right and left foot respectively, f_{jzr} and f_{jzl} are the forces applied to sensor j in z -direction on right and left foot respectively and p_{jr} and p_{jl} are the positions of the sensors on the right and left foot respectively. The force sensors implementation with signal processing board on foot and the calibration software is shown in Fig. 11.

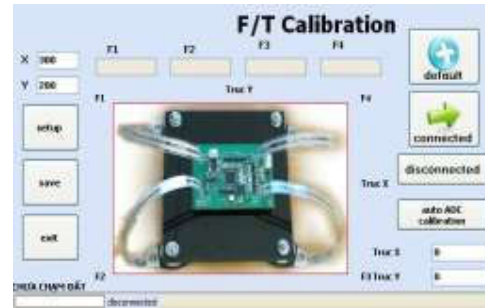


Fig 11. Calibration software of force sensor on foot

When humans are walking they use their inner ear to sense motion and orientation, and when the orientation is felt it is possible to balance. Hence, for HUBOT-1 to be able to walk it is desirable that it is capable of sensing the 3D orientation. For this reason HUBOT-1 is equipped with an IMU which can measure the 3D orientation and accelerations.

6. CONTROL SYSTEM DEVELOPMENT

The system consists of two units, the biped robot and a PC for monitoring. The link between them is through RF communication. The robot control system consists of an embedded computer with OMAP processor running WinCE operating system. The CAN communication interface is used to gather information from sensors and send joint variables to motor drivers as well (Fig. 12). The robot control interface from computer for testing the communication and off-line control is shown in Fig. 13.

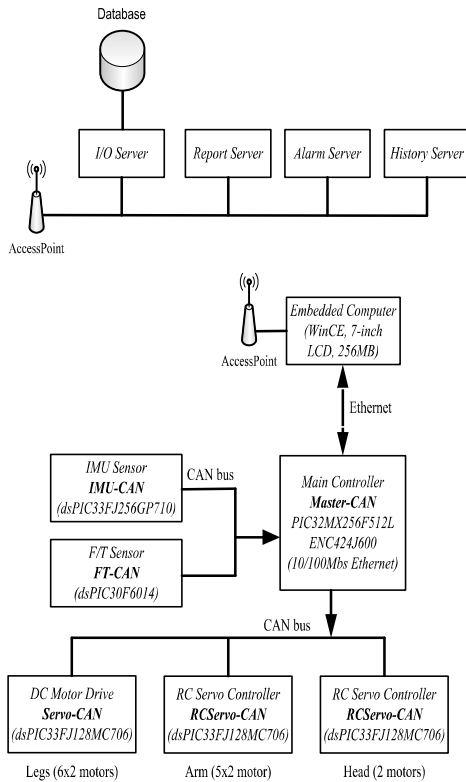


Fig 12. Overall structure of the control system

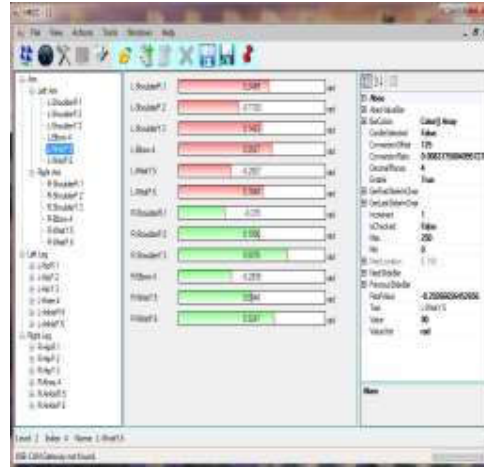


Fig 13. Robot control interface

7. CONCLUSION

In this paper, the design process of humanoid robot HUBOT-1 is presented from mechanical design concept to human walking planning and control system integration. The control strategy in this research is offline motion planning, that is the walking trajectories are calculated beforehand using an external computer and then implemented on the robot as functions describing the trajectories.

The simulation results and testing indicate that walking algorithm can be implemented to the practical robot.

**PHÁT TRIỂN ROBOT GIỐNG NGƯỜI CÓ KHẢ NĂNG BƯỚC ĐI BẰNG HAI CHÂN
- HUBOT-1 THIẾT KẾ ĐẦU TIÊN VÀ NHỮNG KẾT QUẢ ĐẠT ĐƯỢC**

Nguyễn Thanh Nhựt, Phan Huỳnh Lâm, Chung Tấn Lâm

DCSELAB, Trường Đại học Bách Khoa, ĐHQG-HCM

TÓM TẮT: Bài báo trình bày quá trình thiết kế robot người HUBOT-1 từ thiết kế cơ khí, hoạch định quỹ đạo, tích hợp cảm biến và thiết kế bộ điều khiển. Robot được thiết kế có kích thước theo tỉ lệ của người Việt Nam. Phần chân của robot với 12 bậc tự do được xem xét nhằm đạt mục đích bước đi tự nhiên giống người. Quỹ đạo các góc khớp của chân được hoạch định từ quỹ đạo của bàn chân và hông theo tiêu chuẩn cân bằng ZMP. Bộ điều khiển dead-beat được sử dụng để điều khiển bám theo các góc khớp đã tính được. Ngoài ra, các cảm biến IMU và FSR được sử dụng để hồi tiếp các giá trị mong muốn nhằm tính toán và kiểm tra cân bằng cho robot.

Từ khóa: robot người HUBOT-1.

REFERENCES

- [1]. Y. Sakagami, R. Watanabe, C. Aoyama, M. Shinichi, N. Higaki, and K. Fujimura, *The intelligent ASIMO: System overview and integration*, in Proc. IEEE Int. Conf. Intell. Robots Syst., Lausanne, Switzerland, pp. 2478–2483, Oct. (2002).
- [2]. T. Sawada, T. Takagi, and M. Fujita, *Behavior selection and motion modulation in emotionally grounded architecture for QRIO SDR-4XII*, in Proc. IEEE Int. Conf. Intell. Robots Syst., Sendai, Japan, vol. 3, pp. 2514–2519, Oct. (2004).
- [3]. K. Hirai, M. Hirose, Y. Haikawa, and T. Takenaka, *The development of Honda humanoid robot*, in Proc. IEEE Int. Conf. Robot. Autom., vol. 2, pp. 1321–1326, May (1998).
- [4]. K. Erbaturo, O. Kurt, *Natural ZMP Trajectories for Biped Robot Reference Generation*, IEEE Transactions on Industrial Electronics, vol.56, No.3, March (2009).
- [5]. J.J. Craig, *Introduction to Robotics: Mechanics and Control*, 2nd ed. (Addison-Wesley Publishing Company 1989), p.129.
- [6]. Q. Huang, K. Yokoi, S. Kajita, K. Kaneko, H. Arai, N. Koyachi, and K. Tanie, *Planning Walking Patterns for a Biped Robot*, IEEE Transactions on Robotics and Automation, Vol. 17, No.3, June, (2001).
- [7]. Vukobratovic, M. and Borovac, B., *Zero-Moment Point - Thirty Five Years of Its Life*, Int. Journal of

Humanoid Robotics, Vol.1, No.1, pp.
157-173, (2004).

walking robot Hubot-1, VCM
National Conf., (2010).

- [8]. TN Nguyen, HL Phan, TL Chung,
Development of a humanoid biped